Delaunay Triangulations and Stereographic Projections

Alan Saalfeld
Department of Civil and Environmental Engineering and Geodetic Science
The Ohio State University; Columbus OH 43210-1275
Email: saalfeld.1@osu.edu

Abstract

After describing Delaunay triangulations of vertices on a sphere and in a plane, we prove that every Delaunay triangulation of vertices on a sphere corresponds to the Delaunay triangulation in the plane of any stereographic projection of the spherical triangle vertices. We then exploit this correspondence to build robust algorithms for Delaunay triangulations in the plane or on the sphere. We also describe a collection of "fisheye" conformal transformations of the sphere that are the composition of one stereographic projection with the inverse of another stereographic projection.

Keywords: Map transformations, Voronoi diagrams, partitions, conformal mapping

Introduction

Delaunay triangulations arise naturally and frequently in mapping applications and in spatial data management problems. Triangulated Irregular Networks (TINs) (Mark, 1997) have long played an important role in elevation mapping (Peucker, 1978); and Delaunay triangulations offer many computational and theoretical advantages over other TIN decompositions. A Delaunay triangulation in a plane also is the dual graph (or topological dual) of a Voronoi diagram, a fundamental spatial data structure for facilitating nearest neighbor queries and point searches (Bern, 1997). The Voronoi diagram may be built from the Delaunay triangulation in linear time and vice versa. Often the two plane graphs are built simultaneously (see Figure 2), since the Voronoi vertices are the circumcenters of the triangles of the Delaunay triangulation; and the circumcenters are handy (and thus are often computed) to maintain the Delaunay triangulation for dynamic point sets.

Delaunay triangulations and Voronoi diagrams in the plane each have counterparts on the sphere. On the sphere, edges are minor arcs of great circles (like the line segments in the plane, these arcs are also geodesics). As in the plane, Voronoi edges lie on perpendicular bisectors of Delaunay edges in the sphere. The associated structures naturally are also called "Delaunay triangulations" and "Voronoi diagrams" of the sphere, respectively (see Figure 1). There is mathematical software (Renka, 1984) for Delaunay triangulations on the sphere and even at least one commercial mapping product available that partitions the globe into Delaunay triangulations and Voronoi diagrams[1] (Lukatela, 1987).

While there are many ways to associate points on a region of the sphere with points in the plane (any map projection, of course, is just such an association), it is not immediately clear that any of the associations of points extend to associations of their triangulations (i.e., extending an association to the triangulations would mean that the corresponding edge sets each triangulate their respective spaces). Edges themselves are not generally associated point for point. Great circle arcs usually do not project to straight lines under arbitrary projections. The one projection that sends all great circles to straight lines, the central azimuthal or gnomonic projection, does not preserve relative distances along those lines.

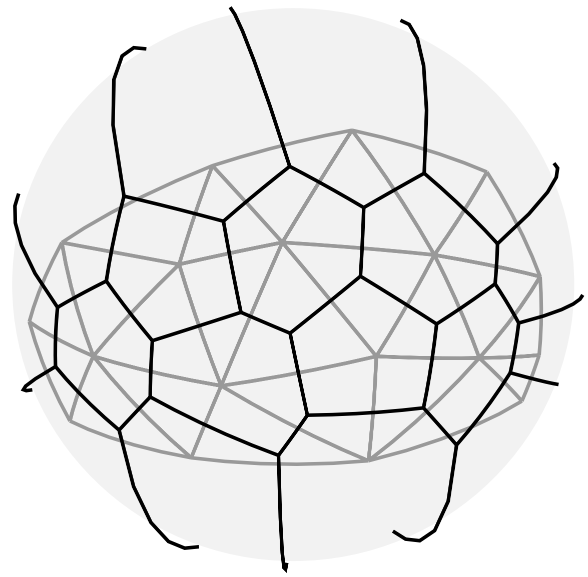

Figure 1: Delaunay triangulation (gray) and its dual Voronoi diagram (black) on a sphere

Delaunay Criteria

In the plane, Delaunay triangulations are characterized by the empty circumcircle property. A triangulation is Delaunay if the interior of the circumcircle of each of its triangles contains no vertices of the point set. On a sphere any circle is the intersection of a plane slicing through the sphere. Each circle then bounds two "bubbles," a larger and a smaller bubble (see Figure 3). The naturally equivalent condition to the empty circumcircle property in the plane is the empty bubble property on the sphere.

In other words, the smaller of the two "bub-

[1] http://www.geodyssey.com/hipparchus.html

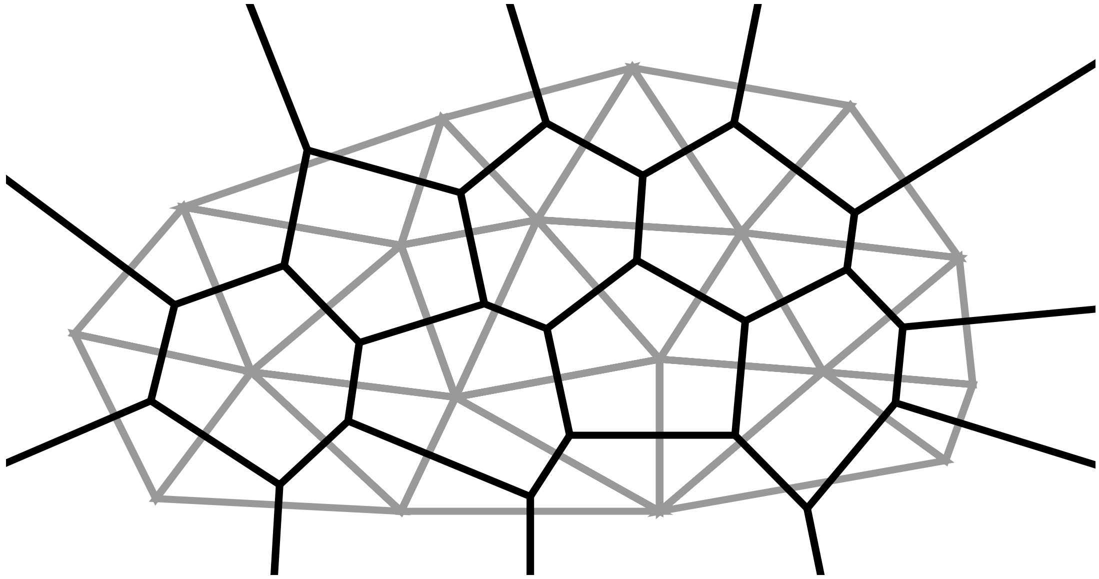

Figure 2: Delaunay triangulation (gray) and its dual Voronoi diagram (black) in a plane

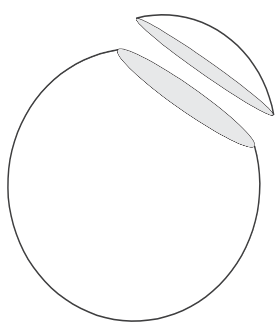

Figure 3: Any circle on the surface of the sphere divides the sphere into a large and a small bubble

bles" formed by the circle on the surface of the sphere passing through the triangle vertices is empty. The bubble will be empty if and only if there are no other vertices (in 3-D space) on one side of the plane that passes through the three triangle vertices. Thus if we replace the great circle arcs with chords of those arcs, we get exactly the edges and vertices of the convex hull of the vertex set. In fact, one may define the Delaunay triangulation of a point set on the sphere to be the convex hull of the point set, then interpret triangular facets of the polyhedron as spherical triangles, as illustrated in Figure 4.

As before, an empty "circum-bubble" signifies that all vertices not belonging to a triangle are on the same side of the plane of the triangular facet. For some triangulations of the sphere, testing sidedness of the plane is a quick and easy test. On the other hand, if the curvature in a region is very slight, then all points will be nearly co-planar; and testing for sidedness may produce inconclusive results (the true or measured distance to the plane may be smaller than the uncertainty of measurements and computations). A simple test for sidedness involves plugging the coordinates of the test point (x_0, y_0, z_0) into the linear expression, $Ax+By+Cz+D$, whose zero-set, $\{(X, Y, Z) \mid AX+BY+CZ+D = 0\}$, defines the plane. If the sign of the evaluated expression is positive, then the point is on one side of the plane; if the sign is negative, the point lies on the other side of the plane. If the region itself is too flat, then the evaluated expression will be too close to zero to say anything definite about its sign. In other words, the computed value involving three multiplications and three additions might have a computable uncertainty that is greater in absolute value than the computed value itself.

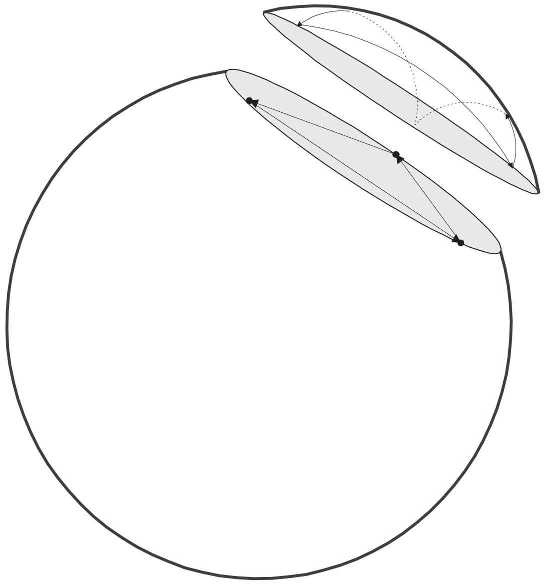

Figure 4: A spherical triangle and its plane (chordal) triangle

In the section on inverse stereographic projections we will describe how to augment curvature locally to permit the application of convex hull methods of computation when the sidedness test would otherwise be inconclusive.

Preserving Delaunay Criteria

What does it mean for a transformation to preserve Delaunay criteria? We have a few possible different interpretations. The first possibility is the preservation of Delaunay edges. Suppose that we are given an arbitrary Delaunay triangulation in a domain space and a transformation from that space to another space, which we call the range space. We might insist, for example, that edges be transformed into edges; and that, furthermore, the resulting edge set in the range space constitute a Delaunay triangulation of the resulting vertex set of that space. This condition turns out to be too constraining—the only transformations that send Delaunay edges to Delaunay edges (as point sets) are similitudes (rigid motions, reflections, scalings, and compositions of those three types of transformations) from the plane to the plane; or rotations and/or inversions from the sphere to the sphere. There are no Delaunay edge preserving transformations between the sphere and the plane. Indeed, the only edge preserving transformations from sphere to plane are gnomonic projections followed by arbitrary perspective or affine transformations of the plane to itself; and none of these composite transformations preserve the Delaunay property (empty circumcircles).

A second possible interpretation is the preservation of the combinatorial triangulation. A combinatorial triangulation of a set of vertices is the collection of vertex triples that correspond to the triangles of the triangulation (or equivalently, a collection of vertex pairs that correspond to the edges of the triangulation). Although each domain edge is not transformed (as a point set) to a range space edge (and neither is each triangle transformed as a point set to a triangle), nevertheless, any triple of vertices and its image triple may be tested to determine if each triple is a Delaunay triangle vertex set in its respective domain or range space. Under this notion of preservation of Delaunay criteria, we have the rather surprising result that *all* stereographic projections from sphere to plane, (and *only* stereographic projections), will satisfy the criteria. In fact, mapping circles (and their interiors) to circles (and their interiors) is precisely the Delaunay test condition that is preserved by stereographic projections (and only by stereographic projections). We, therefore, have the following result:

Theorem 1. *Suppose that the Delaunay triangulation in each of two spaces is characterized by the empty circumcircle property. Suppose further that a transformation between the two spaces sends circles and their interiors to circles and their interiors. Then such a transformation sends a combinatorial Delaunay triangulation of vertices in the domain space to the combinatorial Delaunay triangulation of the corresponding image vertices in the range space.*

Stereographic Projections

A stereographic projection from the sphere to the plane may be described geometrically as follows: Attach a tangent plane Π to the sphere at the South Pole. For any point p on the sphere other than the North Pole, shoot a ray from the North Pole through the point p and continue the ray until it touches a point $\pi(p)$ in Π. Then the association of points, $p \to \pi(p)$, is a (polar or normal) stereographic projection of the sphere (minus the North Pole) onto the plane[2]. An arbitrary (oblique) stereographic projection may be obtained by attaching the tangent plane at an arbitrary point, then projecting rays through the sphere to the tangent plane from the antipodes (opposite point) instead of from the North Pole. Figure 5 illustrates the geometric constructions of stereographic projections.

Stereographic projections are conformal. At any point they have the same scale factor in all directions. The Tissot Indicatrix, an ellipse which describes relative directional distortion at each point is everywhere a circle for conformal maps. Sometimes the property of conformality is described as taking infinitesimal circles to infinitesimal circles[3]. The stereographic projection does even better: it takes *all* circles to circles! For an excellent overview of these and other geometric properties of the stereographic projection, see *Geometry and the Imagination in Minneapolis*, an online collection of handouts (Conway *et al.*, 1991) for a two-week summer workshop entitled "Geometry and the Imagination", led by John Conway, Peter Doyle, Jane Gilman, and Bill Thurston at the Geometry Center in Minneapolis, June 17-28, 1991.

[2]While cartographers describe this projection onto a tangent plane, mathematicians often "project" onto the equatorial plane. The only difference in the images is a scale factor of 2.

[3]The modern description of this property of limits is that the induced linear map of the tangent plane at any point to the tangent plane of the image point is a similitude.

Inverse stereographic projections

The circle preserving properties of the stereographic projection are also enjoyed by its inverse. Not only does every circle on the sphere get sent to a circle on the plane projection surface, but every circle on the plane comes from, or may be lifted to, a circle on the sphere. This guarantees that combinatorial Delaunay triangulations in the plane have a Delaunay counterpart triangulation (and convex hull construction) on any associated sphere as long as the association is derived from some stereographic projection. The sphere size and its point of tangency will determine the extent of the inverse image of the planar region. Smaller spheres will have greater angular extent, as shown in Figure 6.

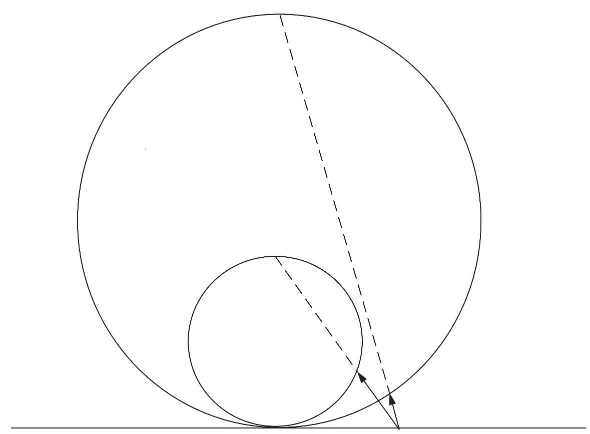

Figure 6: Inverse stereographic projections in cross-section

Given a rectangular map, one may choose a sphere of appropriate size so that the inverse stereographic projection covers a reasonable amount of the sphere, but does not exhibit extreme distortion anywhere. A balanced tradeoff may be achieved by selecting a tangent sphere of diameter equal to one half the diagonal of the rectangular map (see figures 7 and 8). In Figure 8 only triangle vertices are projected. Edges are not projected as point sets. Triangle edges are reconstructed (as great circle arcs) by linking vertices. Voronoi edges are then built as perpen-

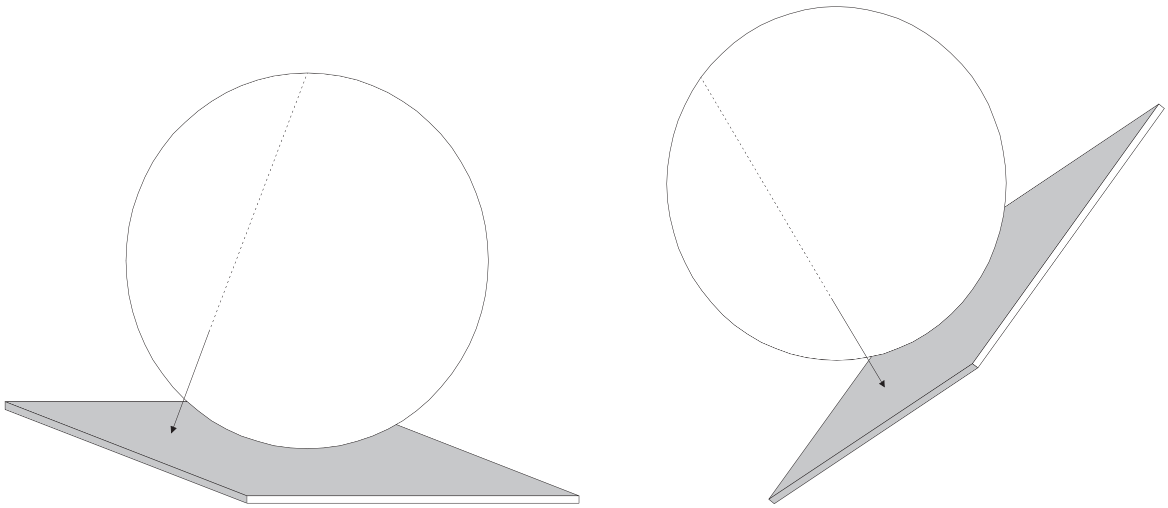

Figure 5: Normal (left) and oblique stereographic projection

dicular bisectors of triangle edges.

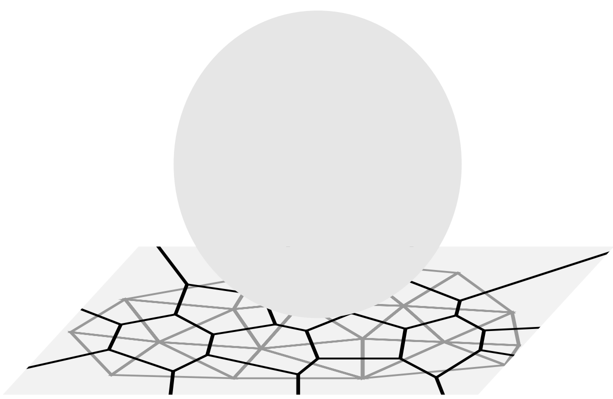

Figure 7: Rectangular region prior to inverse stereographic projection to hemisphere

By attaching the sphere at its south pole so that it is tangent to the map at the center of the map, the rectangle maps entirely to the lower hemisphere, the rectangle corners map to the equator; and the scale factor varies monotonicly from 1:1 at the south pole to 1:2 at the equator of the attached sphere. Thus all length measures of features on the rectangular representation are shrunk by a factor between one-half and one to obtain corresponding feature lengths on the sphere. Moreover, all pairs of points in the rectangle have their geodesic distances reduced by a factor between 1:2 and 1:1 when they are “projected up” onto the lower hemisphere and their separation is measured using the geodesic metric of the sphere. This range of ratios holds for more than geodesics; it holds for all path lengths of paths on the rectangle compared to image path lengths on the hemisphere. Since path length is simply the integral of the norm of the velocity vector along a parameterized path; and since that vector’s norm is transformed (i.e., multiplied) by the local instantaneous map scale in the appropriate direction[4] along the image path, the intermediate value theorem of calculus guarantees that the entire path length gets stretched or shrunk somewhere between extreme local changes of 1:1 (maximum) and 1:2 (minimum).

We may also assess the rate at which the scale is changing by noting that the similar triangles in Figure 9 give us the following precise closed expression for the scale factor everywhere in terms of the latitude ϕ (measured in radians south of the equator):

$$s_\phi = (R + R\sin\phi)/2R = (1 + \sin\phi)/2.$$

[4] Only the location and not the direction matters when assessing scale factors for conformal maps.

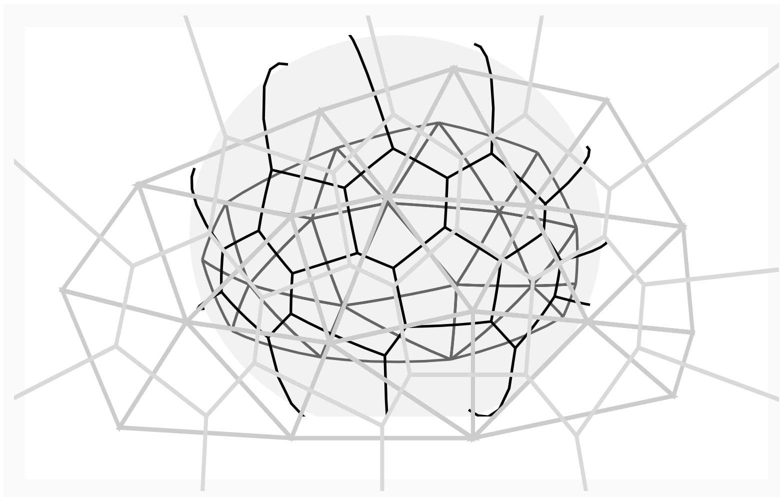

Figure 8: Inverse stereographic projection to hemisphere (as seen through a transparent plane)

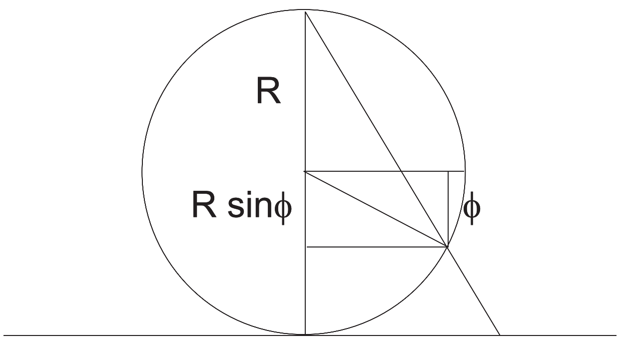

Figure 9: Scale factor as a function of ϕ

From the expression for the scale factor, we see that the rate of change of the scale factor is also a function of the latitude ϕ along meridians and is unchanging along parallels of latitude:

$$\partial s_\phi/\partial\phi = \cos\phi/2; \qquad \partial s_\phi/\partial\lambda = 0.$$

The above analysis of distortion properties guarantees that relative between-point distances are never more than equaled or less than halved when transforming from the rectangle to the hemisphere. Since the rectangle diagonal (of length $D = 4R$, where R is the sphere's radius) is transformed into a semicircle (half of a great circle, or 180°), we conclude that a pair of points on the rectangle separated by a distance d will be separated by an angular great circle distance of at least $(1/2)(d/D)180°$ and no more than $(4/\pi)(d/D)180° = d180°/(\pi R)$. This guaranteed separation can provide a satisfactory assurance that the triangulation points on the hemisphere will be sufficiently far from being coplanar to allow unambiguous determination of the sidedness of other sphere points with respect to cutting planes. Thus the convex hull test can be conducted robustly for points distributed reasonably well on a hemisphere.

Delaunay triangulation of points in a plane rectangular region may be accomplished along the lines of the following pseudo-code:

1. `At the centroid of the rectangle, attach a tangent sphere of diameter equal to 1/2 the rectangle's diagonal.`

2. `Project the triangulation points` $\{p_1, p_2, \ldots, p_k\}$ `from the plane to the hemisphere via the inverse stereographic projection,` π^{-1}.

3. `Insert the points on the sphere` $\{\pi^{-1}(p_1), \pi^{-1}(p_2), \ldots, \pi^{-1}(p_k)\}$ `one at a time. With each insertion` $\pi^{-1}(p_i)$, `update the convex hull of the collection of inserted points. To accomplish this, do the following:`

(a) `Locate the current hull bounding triangular facets for which` $\pi^{-1}(p_i)$ `lies outside the planes of those triangles;`

(b) `Connect` $\pi^{-1}(p_i)$ `to each horizon edge segment to form a new hull triangular facet.`

(c) `Update the coefficients and the sidedness criteria of the convex hull triangular facet bounding planes.`

This pseudo-code does not describe explicitly how to perform the sidedness tests, but there are several observations that may facilitate the tests. First we note that every point on the sphere indeed belongs to the convex hull; hence, each point, when added, will lie outside some previously added facet. If that facet has the following equation to define its plane: $\{(X, Y, Z) \mid AX+BY+CZ+D=0\}$, then any (X, Y, Z) that evaluates to a number with the opposite sign of D will lie outside the plane of the facet. This is easily seen to be true by noting that the center of the sphere (which is clearly an inside point) evaluates to D because all other terms drop out ($X=Y=Z=0$). Hence outside points must evaluate to a number of the opposite sign.

Conformal Globe Transformations

The inverse of a conformal mapping is necessarily a conformal mapping as well. The composite of two conformal mappings is a conformal mapping. We already saw in the section on inverse stereographic projections that an inverse stereographic conformal mapping from the plane to the sphere has many important properties that guarantee that the function does not change scale too rapidly. On the hemisphere at which a tangent plane is attached, for example, the range of scales only varies between 1:1 (at the point of tangency) and 1:2 (90° from the point of tangency). This relatively small variation results in reasonable lower bounds and upper bounds for distortion in an extended area of interest. The rate of change of the scale is itself also well-behaved, ranging from $0 = \cos(\pi/2)$ at the point of tangency to $1/2 \;\; (= (\cos 0)/2)$ at 90° away. We note that the general study of arbitrary conformal mappings between two spheres belongs historically to the realm of complex variables and holomorphic functions on the Riemann sphere (which is precisely the analytical equivalent of the complex plane augmented with a point at infinity (Kodaira, 1984)). Conformal transformations are unusual in that they really have no flexibility in the following sense: once a function is defined on any open neighborhood, however small, and the function is required to be conformal on its domain, then the function is completely determined everywhere. Another way of saying this is that if two conformal functions agree on any arbitrarily small neighborhood, then they agree on their entire domains.

Fisheye Conformal "Global-grams"

The conformal functions from sphere to sphere that consist of stereographic projections followed by inverse stereographic projections are just one kind of conformal sphere-to-sphere mapping. However, these functions have demonstrably good analytical properties. First these functions always take bubbles to bubbles. By regarding the intermediate mapping to a plane, we see that circles are always preserved to and from the sphere. Hence the composite sphere to sphere maps send circles to circles (and their interiors to interiors). In fact, given the point p in the interior of any bubble B, we may send the bubble B exactly onto the southern hemisphere by a conformal transformation that also sends p to the south pole (Kodaira, 1984). This conformal mapping will be unique up to rotation. Since any bubble may be transformed conformally to the southern hemisphere, any bubble may be transformed conformally to any other bubble. More-

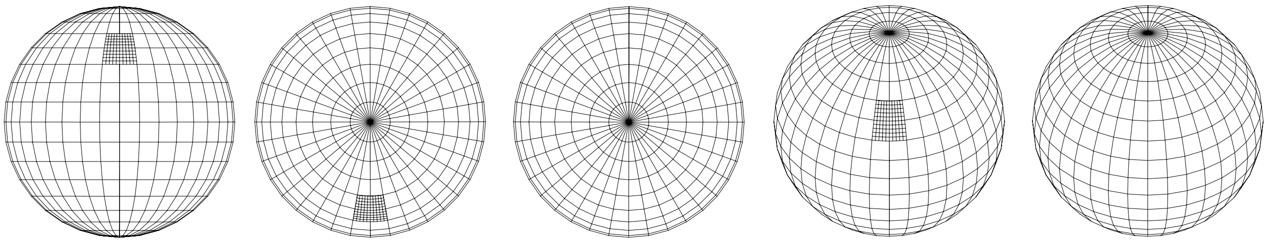

Figure 10: Five orthographic views of the earth's graticule (10° spacing in latitude and longitude) from space with viewpoints along a single meridian taken above points on that meridian at the equator, the poles, latitude 40°N, and its antipodes. A finer (2°) grid is drawn centered at 40°N.

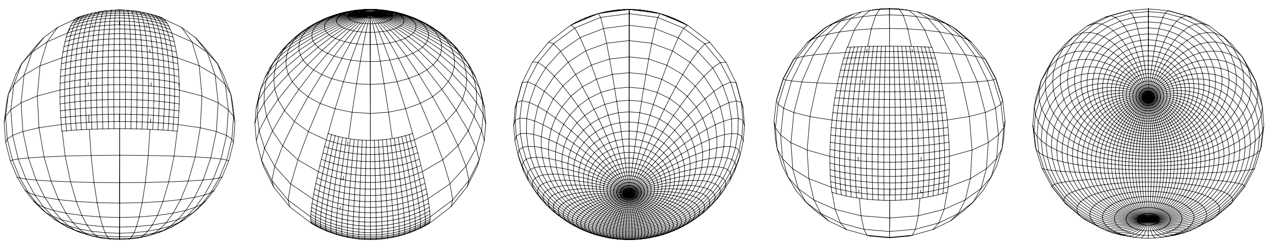

Figure 11: Five corresponding orthographic views of a "Fisheye global-gram" (5° graticule), all taken above the meridian containing the magnification (4X) point at latitude 40°N (1° fine grid)

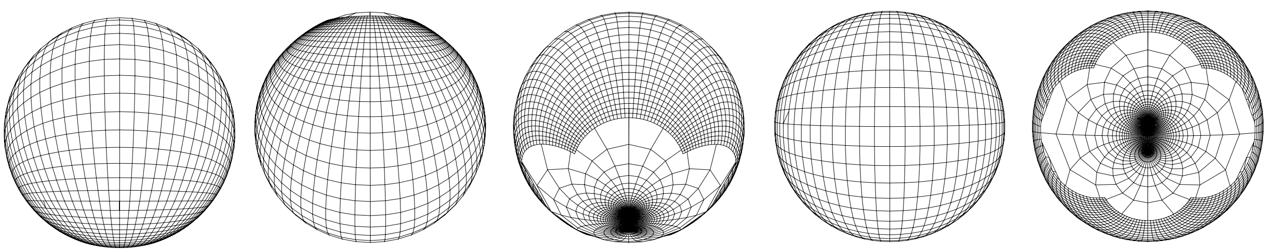

Figure 12: Five corresponding orthographic views of a "Fisheye global-gram" (5° graticule), taken above the meridian containing the magnification (20X) point at latitude 40°N (1/2° fine grid)

over, if both bubbles are smaller than a hemisphere and bubble central point goes to bubble central point, then the largest and smallest scale factors of the transformation of the two bubbles have a ratio no greater than 1:2. This last observation permits the local magnification of a point and its surrounding area on a globe with a reasonably gradual diminishing of scale away from the focal point. The "global" or 3-D equivalent of cartograms, maps that exaggerate areas unevenly, may be built to enlarge circular regions on a sphere at the relative expense of other regions (compare figures 11 and 12 with Figure 10). All of the 15 views in figures 10, 11 and 12 have the prime meridian appearing as (part of) a central vertical line. The finer gridded region of interest is always split by this line (although the region cannot be seen in the third and fifth panels of each row because the region center is opposite the viewer). Because the transformations stretch the prime meridian unevenly, the corresponding figures in each vertical column always keep the center of the detailed region (latitude 40° N) in the same spot relative to the viewer.

Much like the stylized "map" on the famous cover of the New Yorker magazine, one could build a globe with an entire hemisphere (or more) occupied by the area of New York or of any other city or state or other region. Unlike most cartograms, however, the conformal "global-gram" exhibits readily quantified distortion properties: no angle distortion (lines of latitude and longitude always cross at right angles), radial distortion (scale diminishes in a distance dependent manner away from the focal point), geodesics are circles (great circles if measured from focal point).

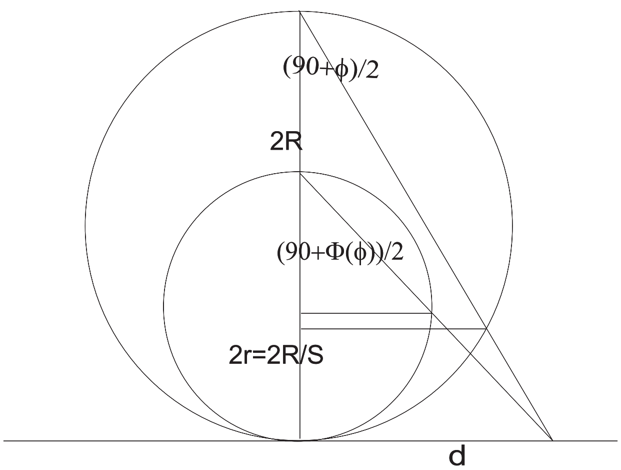

Figure 13: Relationship of parallels of latitude

Suppose that we wish to enlarge the region about the point p by a factor of S on a sphere of radius R. We may accomplish this by the following:

1. `Compute a rotation` Γ `that sends` p `to the south pole of the sphere of radius` R.
2. `Compute the transformation of latitudes` $\Phi(\phi)$ `that corresponds to the conformal transformation that is the composite function of the two requisite functions, a stereographic projection from the sphere of radius` R `and the inverse stereographic projection to the sphere of radius` $r = R/S$.
3. `Apply` $\Gamma^{-1} \circ \Phi \circ \Gamma$ `to all points on the sphere.`

The before and after effects of the transformations may be seen in figures 10 (before), and 11 and 12 (after), respectively.

The computation of Φ is illustrated in Figure 13. We assume that ϕ goes from $-90°$ at the south pole to $+90°$ at the north pole. Since inscribed angles are equal to one-half the subtended arc, we see that the inscribed angles at the north poles of circles of radius R and $r = R/S$ respectively are $(90° + \phi)/2$ and $(90° + \Phi(\phi))/2$. If we let d be the distance of the projected point from the tangent point in the plane (shown as a horizontal line in cross-section), then we have the following:

$$\begin{aligned} \tan((90° + \phi)/2) &= d/(2R); \\ \tan((90° + \Phi(\phi))/2) &= d/(2r); \\ r &= R/S. \end{aligned}$$

Thus we have:

$$S \tan((90° + \phi)/2) = \tan((90° + \Phi(\phi))/2).$$

From this relationship we may explicitly compute the latitude transformation:

$$\Phi(\phi) = 2 \arctan(S \tan((90° + \phi)/2)) - 90°$$

If we solve the relationship in terms of the co-latitudes, the angle along a meridian measured from the south pole, $\chi = 90° + \phi$ and $\Xi(\chi) = 90° + \Phi(\phi)$, then we have the simpler expressions

$$\begin{aligned} \tan(\chi/2) &= d/(2R); \\ \tan(\Xi(\chi)/2) &= d/(2r); \\ r &= R/S. \end{aligned}$$

From this relationship we may explicitly compute the co-latitude transformation:

$$\Xi(\chi) = 2 \arctan(S \tan(\chi/2))$$

Demonstrating "Global-grams"

A web site[5] with geometric Java applets has been set up in the Ohio State University Department of Civil and Environmental Engineering and Geodetic Science to illustrate mapping algorithms and transformations. Computer graphics (in the form of animated `.gif` files) to illustrate fisheye conformal transformations on spheres have been added to the site. Maple programming code for generating the animations is also available there for downloading.

References

1. Bern, Marshall, "Triangulations," in *Handbook on Discrete and Computational Geometry*, J. Goodman and J. O'Rourke, eds., CRC Press, 1997.

2. Conway, John; Peter Doyle; Jane Gilman; and Bill Thurston, "Geometry and the Imagination in Minneapolis," an online collection with URL `http://www.geom.umn.edu/docs/doyle/mpls/handouts/handouts.html`, Minneapolis, June 17-28, 1991.

3. Kodaira, Kunihiko, *Introduction to Complex Analysis*, Cambridge University Press, 1984, London.

4. Lukatela, Hrvoje, "Hipparchus Geopositioning Model: An Overview," AutoCarto/8, 1987, Baltimore.

5. Mark, David, "The history of Geographic Information Systems: Invention and reinvention of triangulated irregular networks (TINs)," *Proceedings of GIS/LIS '97*, Cincinnati, October, 1997.

6. Peucker, T. K., Fowler, R. J., Little, J. J., and Mark, D. M., 1978, The triangulated irregular network. Proceedings, American Society of Photogrammetry, Digital Terrain Models Symposium, St. Louis, Missouri, May 9-11, 1978, pp. 516-40.

7. Renka, R.J., "Interpolation of data on the surface of a sphere," *ACM Transactions on Mathematical Software*, 10, 417-436, 1984.

[5] `http://gscgas.eng.ohio-state.edu/resources/index.html`

Alan Saalfeld is assistant professor in the Geodetic Science program of the Department of Civil and Environmental Engineering and Geodetic Science at the Ohio State University. His research focuses on mathematical cartography and algorithms and data structures for spatial databases.